Techno-computing Journal 1(1) 27–41(2025)
https://doi.org/10.71170/tecoj.2025.1.1.27-41
Research Paper

Performance of hybrid ANFIS and numerical simulation to predict the effect of steel fibre on compressive strength of concrete

Daha S. Aliyu [1,4*], Haruna Ibrahim[2], Mahmoud M. Farouq [3,4], Hafizu Hamza Ali [5]

[1] *School of Engineering, Newcastle University Upon Tyne, NE1 7RU, United Kingdom*
[2] *Department of Civil Engineering, Cerge Paris University, Neuville-sur-Oise, France*
[3] *School of Architecture, University of Nottingham, United Kingdom*
[4] *Department of Civil Engineering, Aliko Dangote University of Science and Technology, Wudil*
[5] *School of Technology, Kano State Polytechnic, Nigeria*
Corresponding Author Email: engrshanono@gmail.com

Abstract

The growing demand for high-performance concrete with enhanced mechanical properties calls for innovative mix designs and accurate predictive tools. This study uses varying formulations to investigate the mechanical performance, particularly compressive strength, of high-performance steel fiber-reinforced concrete (HP-SFRC). Key parameters include water-to-binder ratios (w/b) of 0.35, 0.40, and 0.45; silica fume as a partial cement replacement at 10% and 15%; and steel fiber volume fractions (Vf) of 0%, 0.5%, 1.0%, and 1.5%, with fiber aspect ratios of 80 and 40. Results demonstrate that incorporating silica fume and steel fibers enhances compressive strength, with the most notable gains at Vf = 1.5% attributed to improved stress transfer within the matrix. An adaptive neuro-fuzzy inference system (ANFIS) model was developed and trained on experimental data to improve prediction accuracy. The ANFIS model exhibited superior performance over conventional models, providing more accurate and reliable predictions. Multiple linear regression (MLR) models were also evaluated for predictive ability. While MLR models offered reasonable estimates, they were consistently outperformed by the ANFIS model. This study contributes to optimizing HP-SFRC formulations by highlighting the synergistic effects of silica fume and steel fibers on compressive strength. It underscores the potential of machine learning tools like ANFIS in predictive modeling for advanced construction materials.

Keywords: High-performance concrete, Micro-silica, Multiple linear regression, Neuro-fuzzy inference system, Steel fiber reinforced concrete

1. Introduction

Concrete is a widely used and robust construction material for various infrastructure applications such as building structures, bridges, and sewage pipes due to its durability. Despite its high compressive strength, concrete's ability to resist tension and flexural loads is often restricted [1], [2]. However, a new approach is replacing the conventional approach of using mild steel reinforcement as the sole method to address these weaknesses. Researchers like [1], [3] [4] have explored other types of fibers, such as steel, glass, and polypropylene, and their combinations as potential alternatives to enhance concrete's tensile and flexural strength. Numerous investigations have been carried out to examine the impact of steel fibers on the compressive strength of test samples [5], [6]. For instance, Yoo and Yoon, [6] found that including steel fibers did not significantly elevate the compressive strength of concrete. For instance, the compressive strength results for samples with a reinforcement ratio of 1.5% were 201 MPa for the control specimen and 211 MPa for the test specimen. Wu et al. [5] and Lee et al. [7] noted that

(Received 15 Nov 2024; revised 29 Nov 2024; accepted 2 Jan 2025; first published online 23 March 2025); Journal homepage https://technocomputing.org/index.php/tecoj

the addition of steel fibers had only a minor influence on the compressive strength of concrete specimens. Lee et al. (2017) [7] observed a mere 12% enhancement in compressive strength by adding 0.9% steel fibers.

The findings of experiments conducted by [7], [8] Yoo et al. demonstrate that incorporating steel fibers significantly improves the flexural strength of test samples. [8] observed a 20% increase in flexural strength and a ductile failure mode due to the crack-bridging effect of steel fibers. He discovered that the equivalent flexural strength ratio, representing the ratio of the first peak strength to the energy absorption capacity, improved by 22% with the addition of steel fibers. These outcomes indicate that steel fibers enhance the samples' flexural strength and energy absorption capacity. Research has shown that fuzzy logic is an easy-to-use tool that allows rules to be created based on experience, and fuzzy logic models can explain the relationship between input and output in simple language, which is especially useful when the connection between them is not straightforward. Several researchers, including [9] employed fuzzy logic and neural networks to investigate the impact of additives (e.g., low lime concrete and fly ash) on various properties of concrete, including compressive and flexural strength. The study's findings demonstrated that fuzzy logic could accurately predict the compressive strength of concrete test specimens, and the statistical analysis revealed an RMS value of 0.28. Moreover, neural networking also successfully generated an RMS value of 1.79.

Furthermore, the Fuzzy model exhibited slope and intercept values of 0.9764 and 0.5842, respectively. In a study conducted by Thamma, [10], generate expression programming that accurately forecasts the compressive strength of cement mortar, yielding an RMS value of 1.4956. Similarly, Topçu and Saridemir, [11] utilized fuzzy logic and artificial neural networking to predict the compressive strength of concrete, achieving an RMS value of 2.02. The linear fit of the equation provided a slope value of 0.9824 and an intercept value of 0.6354. Based on the statistical analysis, both models demonstrated satisfactory and reliable outputs. A research project was conducted to investigate the mechanical behavior of HP-SFRC with different w/b ratios ranging from 0.45 to 0.35 and steel fiber volume fractions ranging from 0 to 1.5% (RI = 0 - 3.88), along with 10 and 15% silica fume replacements. Equations were formulated to predict compressive and flexural strength, accounting for the variations in size, shape, and length of the specimens. Furthermore, a power relationship between compressive and flexural strength was developed and compared to previous research and the American Concrete Institute model [12]. Finally, experimental data from earlier studies verified the proposed model's accuracy.

To ensure the safety and advancement of construction projects, a computational analysis was conducted to simulate the compressive strength of High-Performance Steel Fiber Reinforced Concrete (HP-SFRC). This analysis considered eight input parameters related to the mixture proportions. A machine learning framework was incorporated to develop a predictive model for compressive strength to address the challenge of determining the strength of HP-SFRC in situ, which is influenced by site-specific and ambient conditions. The model utilizes the known mixture proportions as inputs to estimate the compressive strength of HP-SFRC. This approach was adopted due to the complexities involved in accurately determining the strength on-site, as indicated by Sofi et al., [13]The article's primary aim is to investigate the effects of silica fume content and steel fiber volume fractions on the compressive strength and mechanical performance of HP-SFRC. It also aims to develop predictive models for HP-SFRC's compressive strength using machine learning techniques, specifically an adaptive neuro-fuzzy inference system (ANFIS), and compare their performance with traditional multiple linear regression (MLR) models.

2. Material and Methods

2.1 Materials and Mixture Proportions

Ordinary Portland cement of 53 grade with a 28-day compressive strength of 54.5 MPa and a specific gravity of 3.15, along with silica fume as a supplementary cementitious material, was employed in the study. The silica fume had a specific surface area of 23000 m2/kg, a specific gravity of 2.25, and a fineness (as determined by residue on a 45 μm sieve) of 2%. The micro-silica was found to consist of 88.7% silicon dioxide, 0.9% carbon, and 1.8% loss on ignition and was compliant with ACI 234R-1996

[14]. The research used a fine aggregate of river sand that passed through 4.75 mm and conformed to grading zone II of IS: 383-1978 (Standard, 2003) [15]. A coarse aggregate of crushed blue granite stones with a maximum size of 12.5 mm was also employed. A high-range water reducer admixture made of locally available sulfonated naphthalene formaldehyde condensate with a specific gravity of 1.20 was added to the mixes. Furthermore, crimped steel fibre with the physical properties given in Table 1 were implemented.

***Table 1**: Physical properties of round crimped steel fibre*

Fibre	Fibre diameter	Fibre length	Fibre wavelength	Aspect ratio l/d	Ultimate tensile strength fu	Elastic tensile strength Ef
Crimped round fibre	0.9mm	35 and 26mm	0.8mm	80 and 40	1200Mpa	200Gpa

Following the guidelines and specifications of ACI 211.4R–93 [16] sixteen series of high-performance steel fibre-reinforced concrete (HP-SFRC) mixes were formulated, and the mixture proportions used in this investigation are listed in Table 2. Each mix had water to binder ratio (w/b) and a fibre volume fraction (Vf) of 0.5, 1.0, or 1.5% by volume of concrete. Additionally, a superplasticizer with a dosage range of 1.75 to 2.5% by weight of binder was added to the mixes. To evaluate the performance of the HP-SFRC mixes. three cylinders 150 diameters × 300 mm height and three prisms 100 × 100 ×500 mm was produced for each mix and cured at 27 ± 2 ◦C in water.

2.2 Methods of Testing

A minimum of three samples were tested to calculate the average compressive strength. The compressive strength of the samples was tested following the [17] standards using a servo-controlled compression testing machine that applied a 14 MPa/min load. Similarly, the flexural strength (Modulus of rupture) test was conducted following the [18]standards and [19]by placing the samples on a supported span of 400 mm and loading them with a third-point loading on a 100 kN closed-loop hydraulically operated Universal Testing Machine at a 0.1 mm/min deformation rate. All the samples were cured in a laboratory setting before testing and retrieved and conditioned just before the test.

2.3 Dataset and Preprocessing

The dataset used in this study comprises 241 records collected from both experimental work and previous studies on high-performance steel fiber-reinforced concrete (HP-SFRC), including sources such as Liao et al. (2015a) and others [20], [21]. Each record includes eight input variables: cement content (385.3–679 kg), coarse aggregate (903–1295 kg), fine aggregate (365–902 kg), water (119.2–221 kg), water-to-binder ratio (0.35–0.45), superplasticizer content (0–30.08 kg), silica fume content (0–120 kg), and steel fiber volume fraction (0–2.0%). The target variable is compressive strength, ranging from 43.6 to 100 MPa. Outliers related to non-standard curing conditions or extreme material properties were removed to ensure data quality. All input features were normalized for preprocessing to a [0, 1] range using min-max scaling to account for varying scales. To streamline analysis, the variables were categorized into four groups—cement and water content (cement, water, silica fume, w/b ratio), aggregate content (fine and coarse aggregates), superplasticizer dosage, and fiber volume fraction. Composite features were generated for each group to reduce input dimensionality and enhance model efficiency, particularly for the Adaptive Neuro-Fuzzy Inference System (ANFIS). Finally, the dataset was split into training and testing subsets to evaluate model performance, with the training set used for model development and the testing set reserved for validation.

$$zi = \frac{\mathrm{di}-\min(\mathrm{d})}{\max(d)-\min(d)} \quad (1)$$

where di represents the actual value, $max(d)$ and $min(d)$are the maximum and minimum values of each feature.

2.4 Compressive Strength

The ML algorithm described in this passage is designed to ascertain the compressive strength of HP-SFRC by looking at eight factors. Unlike traditional methods like multiple linear regression, ML can analyze linear and non-linear relationships between data, allowing for easier physical interpretation [22]. It is also noted that ML has a higher testing accuracy than traditional methods. Additionally, it can store complex relationships between strength properties and mix design for HP-SFRC, which can be revised with newly acquired data. Consequently, the aim is to figure out the compressive strength of HP-SFRC by considering the mixed ingredients and quantities. Limiting the number of ML inputs is necessary to avoid a situation where the parameters to be learned are more than the number of training samples [23]. To accomplish this input-number control, the 8 elements (i.e., the attributes seen in Figure 1) are categorized into 4 groups. These attributes are normalized into the 0 to 1 range and added up in each group to obtain the cement and water feature, the aggregate feature, the superplasticizer content, and the fibre volume fraction, respectively. For instance, when calculating each concrete sample's cement and water feature, each attribute (w/c ratio, cement, silica fume, and concrete water) is normalized into 0 to 1 following Equation (2). Subsequently, the normalized w/c ratio, cement, silica fume, and concrete water are combined as the cement and water feature.

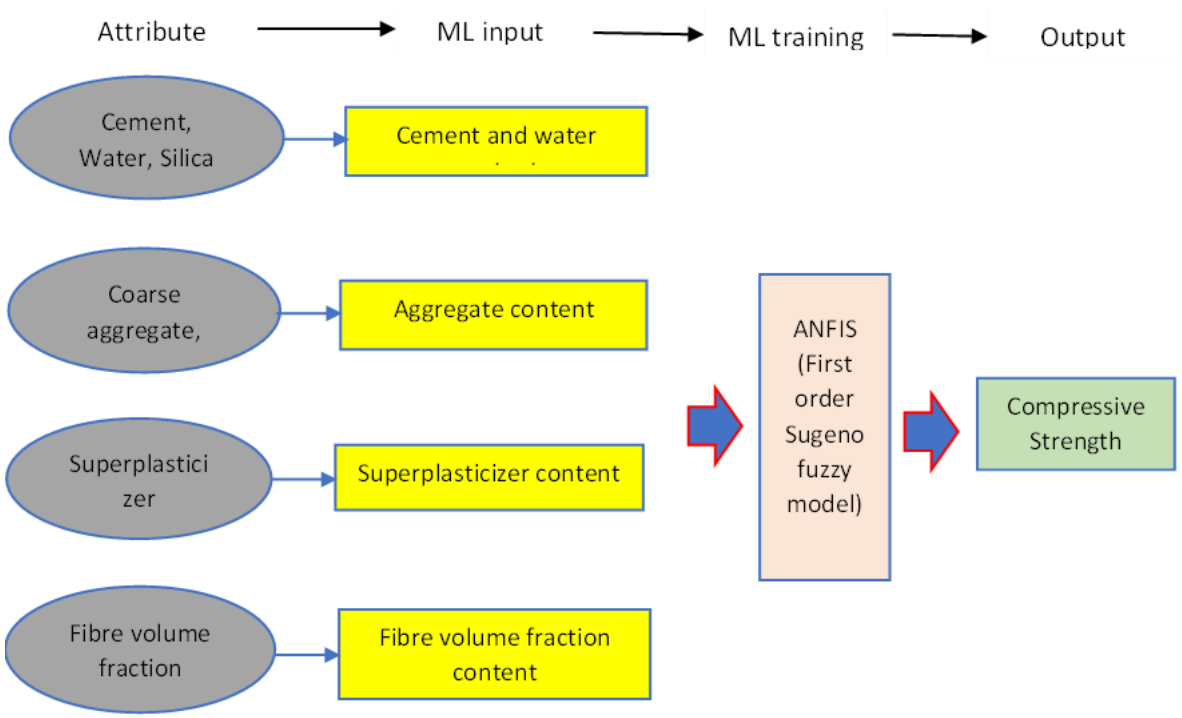

***Figure 1**: Determination of Compressive strength Using ML algorism*

However, [24] employed similar data processing techniques and summarized the normalization process. Cement, water, aggregate, superplasticizer content, and fibre volume fraction were used as the inputs for machine learning to estimate the compressive strength of the HP-SFRC. An ANFIS system has been selected to investigate a non-linear system since it has had numerous applications in this area. ANFIS uses a combined learning technique to determine how to adjust the weights to decrease the difference between the actual and predicted outputs, consequently controlling the parameters and assembly of the fuzzy inference system (FIS). ANFIS is a learning system that uses input-output values to map a model. After obtaining a set of parameters for the model, the model output for each pair of training data is compared to the measured values to calculate the discrepancy between the actual and

measured values. The model is finalised when the stopping criterion is reached [28]. For example, assume the FIS has two inputs, x and y, and one output, f. A typical set of two fuzzy "if-then" rules might look like this:

Rule 1: if x is A1 and y is B1, then $f_1 = p_1x + q_1y + r_1$
Rule 2: if x is A2 and y is B2, then $f_2 = p_2x + q_2y + r_2$ (2)

where,A_i, B_i Refer to the membership functions of the inputs and p_i, q_i, r_i Are parameters which can be adjusted during the learning process. The architecture of ANFIS consists of layers and nodes; the square nodes, which are adaptable, hold the adjustable parameters, while the round nodes are fixed with certain functions, for example:
Layer 1: In this layer, every node i is an adaptive node having a node function.

$$O_i^1 = \mu_{A_1}(\chi), \; for \; i = 1,2 \tag{3}$$

Or

$$O_i = \mu_{B_{i-2}}(y), \; for \; 3,4 \tag{4}$$

Where O_i^1 is the membership grade for input $\chi \; or \; y$. The membership function could include Gaussian, Triangular, Trapezoidal, and Gbell membership.

$$\mu_{A_1}(\chi) = e^{\frac{-1}{2}\left(\frac{x - c_i}{\beta_1}\right)^2} \tag{5}$$

Where $C_i \; and \; \beta_i$ are the premise parameters to be optimised using gradient descent?

Layer 2: Every node in this layer is a fixed node, which multiplies the incoming signal and sends the product out given.

$$Q_i^2 = w_i = \mu_{A_i}(x)\,\mu_{B_i}(y), \; i = 1,2 \tag{6}$$

Layer 3: This layer contains circular nodes, which compute the ratio of the firing strengths of the rules.

$$Q_i^3 = \overline{w}_i = \frac{w_i}{w_1 + w_2} \tag{7}$$

Layer 4: Every node *i* in this layer is an adaptive node and performs the consequent of the rules.

$$Q_i^4 = \overline{w}_i f_i = \overline{w}_i\left(p_i x + q_i y + r_i\right) \tag{8}$$

The parameters $p_i, \; q_i, \; r_i$ are consequent parameters to be determined.

Layer 5: The single node in this layer computes the overall output

$$O_i^5 = \sum_i \overline{w}_i f_i = \frac{\sum_i w_i f_i}{\sum_i w_i} \tag{9}$$

It is well known that Jang [25] combines two approaches, gradient descent and least squares, to alter the parameters of the first and fourth layers of the neural network. As the premise parameters remain constant, the output [26], [27] is obtained during the forward pass when the input vector is passed through the network, and the parameters are modified by the least squares method. The result can be written as:

$$f = \frac{w_1}{w_1 + w_2} f_1 + \frac{w_2}{w_1 + w_2} f_2$$
$$= \overline{w}_1 f_1 + \overline{w}_2 f_2$$
$$= \left(\overline{w}_1 x\right) p_1 + \left(\overline{w}_1 y\right) q_1 + \left(\overline{w}_1\right) r_1 + \left(\overline{w}_2 x\right) p_2 + \left(\overline{w}_2 y\right) q_2 + \left(\overline{w}_2\right) r_2 \quad (10)$$

where p_i, q_i *and* r_i and are the consequent parameters

$$f = XW \quad (11)$$

For invertible X Matrix

$$W = X^{-1} f \quad (12)$$

Otherwise, pseudo-inverse is applied to obtain W

$$W = (X^T X)^{-1} X^T f \quad (13)$$

In the backward pass, the error propagates back through the network, and the premise parameters are optimized by gradient descent.

$$a_{ij}(t+1) = a_{ij}(t) - \frac{\eta}{p} * \frac{\partial E}{\partial a_{ij}} \quad (14)$$

where t is the learning epoch, η is the learning rate for a_{ij} and is the number of input patterns.

The parameters are updated using the expression

$$\frac{\partial E}{\partial a_{ij}} = \frac{\partial E}{\partial f} * \frac{\partial f}{f_i} * \frac{\partial f_i}{\partial w_i} * \frac{\partial w_i}{\partial \mu_{ij}} * \frac{\partial \mu_{ij}}{\partial a_{ij}} \quad (15)$$

The function is expressed as

$$E = \frac{1}{2}(f - f^t)^2, \; so \; \frac{\partial E}{\partial f} = (f - f^t) = e \quad (16)$$

where f^t is the expected output and f depicts the fuzzy system output.

$$f = \sum_{i=j}^{n} f_i, \quad \text{considering} \quad \frac{\partial f}{\partial f_i} = 1 \quad (17)$$

$$f_i = \frac{w_i}{\sum_{i=1}^{n} w_i}\left(p_i x + q_i y + r_1\right), \; so, \; \frac{\partial f_i}{\partial w_i} = \frac{\left(p_i x + q_i y + r_1\right)}{\sum_{i=1}^{n} w_i} \quad (18)$$

$$w_i = \prod_{j=1}^{m} \mu_{A_{ij}}, \text{ therefore, } \quad \frac{\partial w_i}{\partial \mu_{ij}} = \frac{w_i}{\mu_{ij}} \quad (19)$$

Hence, the gradient can now be expressed as:

$$\frac{\partial E}{\partial a_{ij}} = e \frac{\left(p_i x + q_i y + r_i\right) - f}{\sum_{i=1}^{n} w_i} \frac{w_i}{\mu_{A_{ij}}} \frac{\partial \mu_{A_{ij}}}{\partial a_{ij}} \quad (20)$$

Or

$$\frac{\partial E}{\partial b_{ij}} = e \frac{\left(p_i x + q_i y + r_i\right) - f}{\sum_{i=1}^{n} w_i} \frac{w_i}{\mu_{B_{ij}}} \frac{\partial \mu_{B_{ij}}}{\partial b_{ij}} \tag{21}$$

3. Results and Discussion

This section discusses the results for modeling compressive strength. The model pattern was designed with the MATLAB toolbox, which was utilized to accomplish this study. This model comprises four inputs, each associated with bell-shaped membership functions. Following a training epoch of one hundred trials, the ANFIS was tested by evaluating the testing data. This association generated sixteen if-then rules and one hundred-four parameters to be learned. Figure 2 illustrates the relationship between the predicted values and the actual compressive strengths for the training and testing datasets. The R^2 is high for both, which indicates that the model is an accurate predictor of the compressive strength of concrete [29]. The root mean squared error (RMSE) between the actual and predicted values is 0.17 for the training data and 0.56 for the testing data. This further demonstrates the precision of the ML model. A multiple linear regression model was generated with the help of the XLSTAT software after studying a set of data that featured 8 parameters. The model (Eq. 23) had a coefficient of determination of 0.87 and was used to estimate the 28-day compressive strength of HP-SFRC. The multiple linear regression model can be expressed as:

y=106.1751 - 65.9815 /cm + 0.06052 C - 0.0049 FA - 0.00782 CA + 0.21315 SF - 0.23387 W - 0.3603 SP + 0.04146 Fiber with (R=0.982) (23)

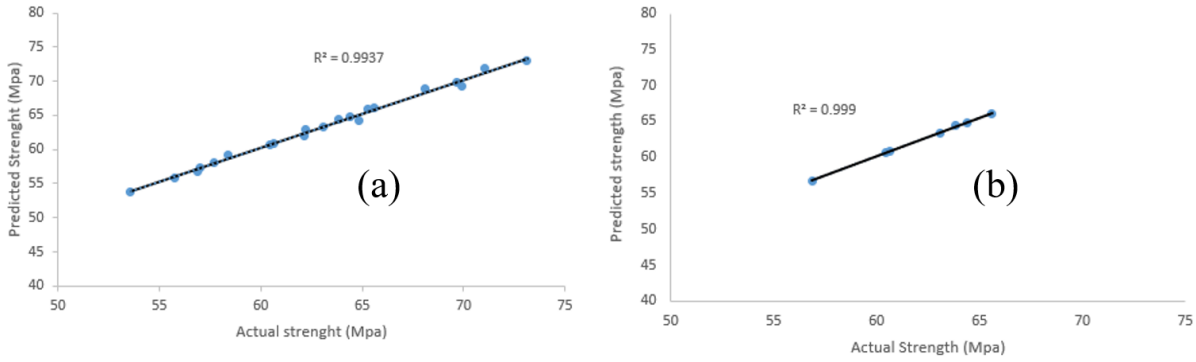

Figure 2: *Correlation between actual compressive strength and predicted compressive strength by the ANFIS (a) training data (b) testing data*

3.1 Mechanical Properties

The study's results showed that incorporating steel fibres into HPC increased the compressive strength by about 12% when the fibre volume fraction was 1.5%. Compressive strengths of plain concrete with w/b ratios of 0.45, 0.40, and 0.35 were 58.4 MPa, 63.84 MPa, and 69.67 MPa, respectively. The compressive strength of HPC with a w/b ratio of 0.45 and a silica fume content of 19% increased by 28.4% compared to the control samples. Increasing the content of supplementary cementitious materials (SCMs) such as micro-silica resulted in improved mechanical properties. The combined effect of silica fume and steel fibers on the compressive strength of HP-SFRC can be seen in Table 2 and Figure 3. As the fibre volume fraction increased, the strength of the HP-SFRC also increased, as seen in Table 3 and Figure 4. An empirical expression was developed to predict the compressive strength (f'cf) of HP-SFRC as a function of fibre volume fraction, Vf (%), for a w/b ratio of 0.4, with an R2 of 0.9233, as shown in Figure 5. This trend was observed to be similar for other HP-SFRCs.

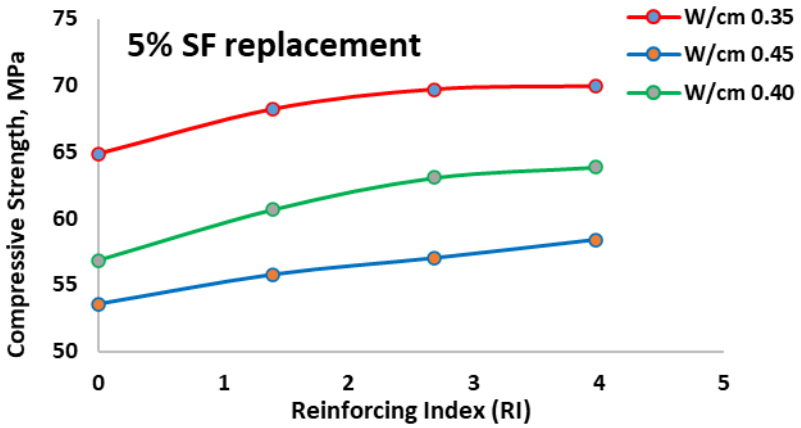

Figure 3: *Effect of fibre reinforcing index (RI) on compressive strength of HPSFRC (5% micro silica replacement)*

The stress-strained behavior of HP-SFRC with a w/b ratio of 0.45 and an SF content of 10% was looked into. The stress-strain relationship of concrete usually features two components - an increasing part up to the peak stress and then a declining part that shows cracking and softening. The main parameters typically used to describe the ascending branch of the curve are the initial tangent modulus, the compressive strength (peak value) and the strain at peak stress. Figure 4 portrays the typical stress-strain (σ–ε) curves for HPC (plain) and SFRC. It can be noted from the stress-strain curves generated in this study that an increase in concrete strength leads to a more curved ascending branch and a steeper drop in the descending part for HPC, and a gradually flatter descent for SFRC. The post-peak region of SFRC shows a gradual decline. However, it still exhibits residual stress even at a strain of 0.015. Fibres' pull-out and fibre bond effects play a prominent role in the post-peak stress-strain behavior of SFRC, and this impact is improved with the addition of SCM due to its strength and filler properties. HP-SFRC compressive toughness is improved as the maximum load is postponed after the peak load because of the bond between fibres and matrix. The post-peak strain values suggest that ductility can be augmented by including fibres in the mix. From the stress-strain curve, it is seen that an increase in the volume fraction of fibers or RI leads to a larger area under the curve, creating a longer-lasting descending part and higher toughness and ductility as exemplified by the post-peak stress-strain behavior of SFRC.

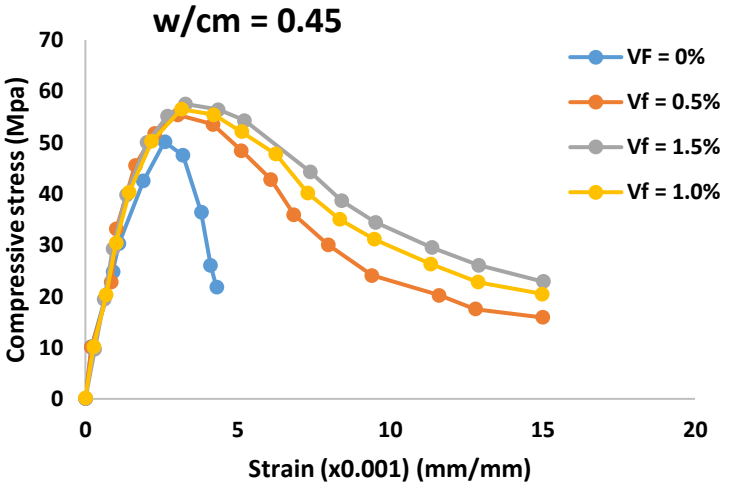

Figure 4: *Stress-strain curves for HPC and steel fibre reinforced concrete (w/cm = 0.45, SF content = 5%).*

Adding steel fibres (Vf = 1.5% or RI = 3.88) to High-Performance Concrete (HPC) was seen to cause a 37% rise in flexural tensile strength, a key indicator of a notable increase in strength and is related to the fibre pull-out effect. During the testing of prism specimens, the failure state was prolonged after the ultimate load, suggesting a significant rise in both ductility and flexural toughness of HP-SFRC. This is in line with the outcomes of previous research studies [30], [31], [32].

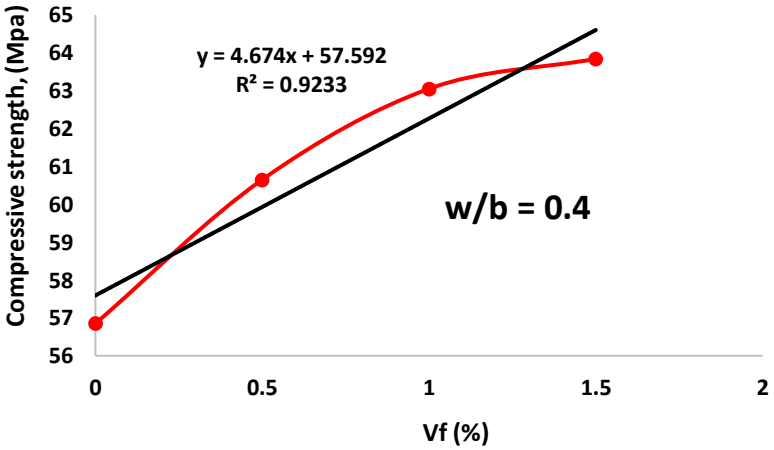

Figure 5: *Effect of fibre volume fraction on compressive strength of HPSFRC (w/cm = 0.40)*

Table 2*: Mix proportion design of HPFRC*

Mix	w/b	FA (kg)	CA (kg)	SF (kg)	B(kg)	W(kg)	SP (%)	SF Vf (%)
M1	0.45	640	1090	44.5	435	196	1.65	0
M1	0.45	638	1087	44.5	435	196	1.65	0.5
M1	0.45	625	1079	44.5	435	196	1.65	1.0
M1	0.45	622	1075	44.5	435	196	1.65	1.5
M1*	0.45	640	1090	67.4	435	196	1.65	0

M2	0.40	636	1090	49.7	483	193	2	0
M2	0.40	627	1086	49.7	483	193	2	0.5
M2	0.40	625	1084	49.7	483	193	2	1.0
M2	0.40	623	1073	49.7	483	193	2	1.5
M2*	0.40	636	1090	74.9	483	193	2	0
M3	0.35	611	1090	56	547	191	2.7	0
M3	0.35	603	1077	56	547	191	2.7	0.5
M3	0.35	595	1073	56	547	191	2.7	1.0
M3	0.35	587	1068	56	547	191	2.7	1.5
M3*	0.35	635	1068	56	547	191	2.7	0

*M1 to M3 and M1 to M3 are Silica fume replacements at 10% and 15%, respectively, SP (%) Superplasticizer in percentage by the weight of binder material, Vf (%) is the steel fiber in the percentage of the total volume of concrete.

Table 3: Mechanical properties result of HPSFRC of fibre =80

Steel fibre				
Mix	**w/b**	**Vf**	**RI**	**f'cf (Mpa)**
M1	0.45	0	0	53.56
M1	0.45	0.5	1.39	55.77
M1	0.45	1	2.68	57.01
M1	0.45	1.5	3.98	58.4
M2	0.40	0	0	56.85
M2	0.40	0.5	1.39	60.65
M2	0.40	1	2.68	63.05
M2	0.40	1.5	3.98	63.84
M3	0.35	0	0	64.86
M3	0.35	0.5	1.39	68.12
M3	0.35	1	2.68	69.91
M3	0.35	1.5	3.98	69.67
M1*	0.45	0	0	57.7
M1*	0.45	1	2.68	62.21
M1*	0.45	1.5	3.98	62.17
M2*	0.40	0	0	60.42
M2*	0.40	1	2.68	64.41
M2*	0.40	1.5	3.98	65.59
M3*	0.35	0	0	65.28
M3*	0.35	1	2.68	71.04
M3*	0.35	1.5	3.98	73.12

*Fibre reinforcing index (RI) = wf *(l/d) and average density of HSFRC = 2425 kg/m.3, Weight fraction (wf) = (density of fibre/density of fibrous concrete) *Vf. Aspect ratio = (l/d); f'cf = 150 Ø x 300 mm cylinder compressive strength of HPSFRC (MPa).

3.2 Compressive Strength Ratio and Fibre Volume Fraction (%)

The graph in Figure 6 demonstrates a linear relationship between the compressive strength ratio of high-performance steel fiber-reinforced concrete (HP-SFRC) and the fibre volume fraction (Vf, %). Empirical equations were generated to predict the strength ratio (f'cf/f'c) of HP-SFRC with a w/b ratio of 0.35-0.45, with a high degree of accuracy (R2 = 0.8699). These equations were obtained using regression analysis using the least-squares method.

$$f'cf/f'c = 1 + 0.067Vf \quad (24)$$

The coefficient of determination, R2 = 0.8699, measures how much of the variation in compressive strength of high-performance concrete (HPC) and high-performance steel fibre-reinforced concrete (HP-SFRC) is explained by the reinforcement parameter, which includes the sample size and a number

of independent variables. Specifically, it is determined that 84% of the variation in strength can be attributed to the fibre volume fraction.

where f'c = compressive strength of HPC (Mpa), f'cf = compressive strength of HP-SFRC (Mpa) and Vf = fibre volume fraction, %.

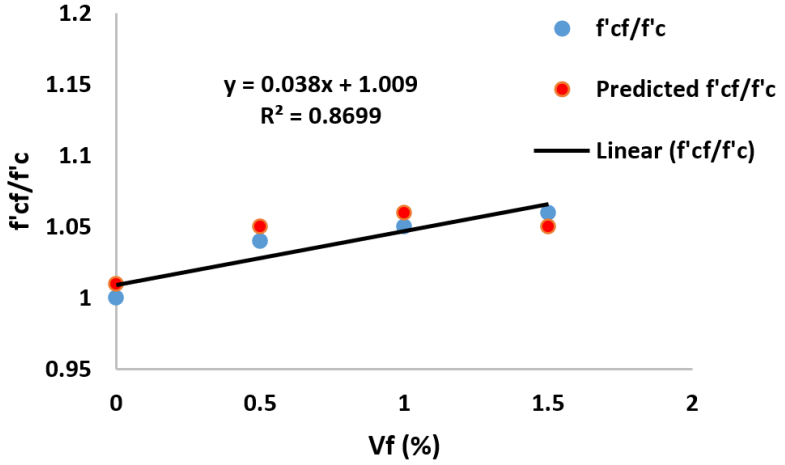

Figure 6: *HPSFRC Vs Fiber volume fraction compressive strength ratios, Vf (%)*

Equation (24) was expanded to analyze the compressive strength of HP-SFRC (f'cf), with the second term representing the contribution of the matrix strength-fibre interaction, which relies on the fibre bond and pull-out characteristics within the matrix. The proposed model was tested on cylinder specimens of HP-SFRC with a fibre aspect ratio (l/d) of 40 (RI = 0 - 2.10), resulting in an average absolute variation of 0.36%. The results of the correlation coefficient (R) and the integral absolute error (IAE) were determined to be 0.92 and 0.97, respectively. The predicted values are documented in Table 4.

Table 4: Compressive strength of HPSFRC and absolute variation by the model of (Eq. (1)) - aspect ratio of fibre (l/d) = 40.

Mix design	**w/b**	**Steel fibre content**		**Compressive strength (Mpa)**		**Absolute % error**
		Vf (%)	RI	Experimental	Predicted	
M2	0.4	0	0	56.85	56.74	0.11
M2	0.4	0.5	1.39	60.65	60.84	0.19
M2	0.4	1	2.68	63.05	63.34	0.29
M2	0.4	1.5	3.98	63.84	64.47	0.63
M2*	0.4	0	0	60.42	60.73	0.31
M2*	0.4	1	2.68	64.41	64.86	0.45
M2*	0.4	1.5	3.98	65.59	66.1	0.51

3.3 Numerical Simulation of Strength

This research conducted a numerical simulation to examine the correlation between the mixture proportions and 28-day compressive strength of HP-SFRC containing micro-silica. The analysis used 8 input elements to assess the compressive strength of HPFRC. The results of the statistical analysis of the data collected from published information are presented in this section. The authors gathered data from 40 different sources to assess the accuracy of the strength model for high-performance concrete (HPC) and high-performance steel fiber-reinforced concrete (HP-SFRC). A total of 250 mixtures from the research studies were assessed. Some samples were removed due to their large aggregate size,

special curing conditions, and other factors not pertinent to the current research. Consequently, a data set of 241 records, each with eight distinct variables, was compiled from the experimental research of this study and Liao et al. [31], [33], [34], [35]. The ranges of components of the data set can be seen in Table 5.

Table 5: Range of data set for HPFRC

Component	Minimum	Maximum
Cement (kg)	385.3	679
Coarse aggregate	903	1295
Fine aggregate	365	902
Water (kg)	119.2	221
Water/binder ratio	0.35	0.45
Superplasticizer (kg)	0	30.08
Fibre volume fraction	0	0.02
Fibre (kg)	0	120
Compr. strength (MPa)	43.6	100

3.4 Comparison of ANFIS vs MLR Model

This study comprehensively compares the performance of ANFIS and MLR models in predicting the HP-SFRC. ANFIS outperformed MLR in both the training and testing phases, achieving R^2 values of 0.92 and 0.87, respectively, indicating strong learning and generalization capabilities. In contrast, MLR achieved slightly lower R^2 values of 0.87 (training) and 0.82 (testing), reflecting its limited ability to capture nonlinear interactions. ANFIS also yielded lower RMSE values, 0.17 for training and 0.56 for testing, compared to MLR's 0.22 and 0.63, confirming higher prediction precision. The key advantage of ANFIS lies in its ability to model complex, nonlinear relationships, such as the combined influence of steel fiber content, water-to-binder ratio, and superplasticizer dosage, with the Sugeno fuzzy inference system dynamically adjusting rules during training. For example, ANFIS effectively captured the nonlinear effect of increasing steel fiber volume fraction (Vf) on compressive strength, unlike MLR, which assumes linearity and struggles with nonlinear trends such as those observed with silica fume content. From a practical standpoint, ANFIS is more accurate and suitable for advanced HP-SFRC mix designs. At the same time, MLR remains useful for preliminary evaluations due to its simplicity and lower computational demand. ANFIS involves 104 adjustable parameters, enhancing its modeling flexibility but requiring more significant computational effort, whereas MLR uses only 8 parameters, offering efficiency at the expense of accuracy. Graphical evaluations showed that ANFIS predictions closely matched actual values with minimal scatter, and 3D surface plots (Figure 7) illustrated interactive effects e.g., a 12% strength increase with steel fiber addition. A parametric study confirmed that steel fibers, alongside silica fume, significantly enhance compressive strength. Empirical equations developed using ANFIS achieved an IAE value of 0.92 and were applicable across varying w/b ratios. In conclusion, integrating steel fibers and silica fume improves HP-SFRC's compressive strength, and ANFIS is a robust predictive tool. It is recommended that ANFIS be used for high-precision applications and MLR for basic assessments, with future research encouraged to develop hybrid models that combine the strengths of both approaches.

Table 6: Comparison of ANFIS and MLR Models

Model	Training Accuracy (R^2)	Testing Accuracy (R^2)	Root Mean Squared Error (RMSE)	Number of Parameters	Key Observations
ANFIS	0.92	0.87	0.17 (Training), 0.56 (Testing)	104	It is highly accurate in training and testing because it can model nonlinear and interactive relationships among input variables. It also provides insights into the influence of individual parameters on compressive strength.
Multiple Linear Regression	0.87	0.82	0.22 (Training), 0.63 (Testing)	8	It performs adequately for linear relationships but struggles to capture the intricate nonlinear effects of variables like fiber volume fraction or superplasticizer dosage on compressive strength.

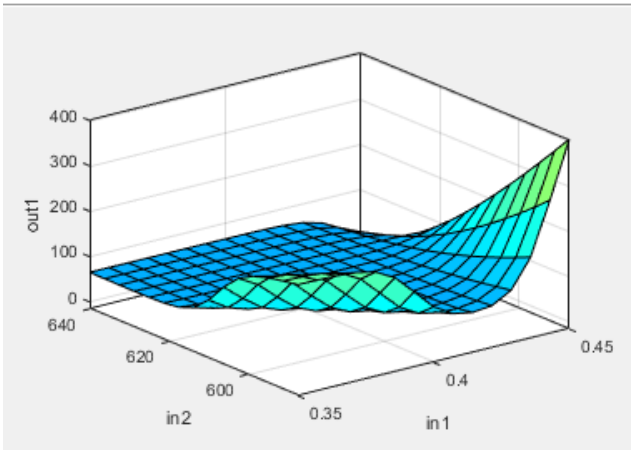

Figure 7: *3D surface plot for HP-SFRC*

4. Conclusion

Based on the experimental and numerical investigation of high-performance steel fiber-reinforced concrete (HP-SFRC) incorporating micro-silica as a supplementary cementitious material (SCM), it was concluded that the inclusion of steel fibers moderately enhances compressive strength while increasing the silica fume (SF) replacement further improves the mechanical performance of the concrete matrix. Empirical equations were developed to predict compressive strength as a function of fiber volume fraction, achieving an impressive index of agreement (IAE) value of 0.92. These equations are independent of specific specimen parameters, utilize non-dimensional variables, and are applicable across a broad range of water-to-binder (w/b) ratios. Additionally, a robust machine learning framework based on an Adaptive Neuro-Fuzzy Inference System (ANFIS) was developed and trained on the dataset, successfully predicting the compressive strength of HP-SFRC with high accuracy, evidenced by RMSE values of 0.17 for training and 0.56 for testing. Based on the outcomes of this study, it is recommended to use ANFIS for high-accuracy predictions, particularly in advanced HP-SFRC mix designs where precise control over mechanical properties is essential. MLR, while less accurate, is suitable for simpler, preliminary analyses or when computational resources are limited. Future research is encouraged to explore hybrid modeling approaches that integrate the computational efficiency of

MLR with the nonlinear modeling capabilities of ANFIS to develop more balanced and scalable prediction tools.

Competing Interests: The authors declare no competing interests.

Data Availability Statement: The supported data associated with this researcher is available upon request from the corresponding author.

References

[1] H. Fathi, T. Lameie, M. Maleki, and R. Yazdani, 'Simultaneous effects of fiber and glass on the mechanical properties of self-compacting concrete', Constr Build Mater, vol. 133, pp. 443–449, Feb. 2017, doi: 10.1016/j.conbuildmat.2016.12.097.

[2] D. Falliano, D. De Domenico, G. Ricciardi, and E. Gugliandolo, 'Compressive and flexural strength of fiber-reinforced foamed concrete: Effect of fiber content, curing conditions and dry density', Constr Build Mater, vol. 198, pp. 479–493, Feb. 2019, doi: 10.1016/j.conbuildmat.2018.11.197.

[3] W. Abbass, M. I. Khan, and S. Mourad, 'Evaluation of mechanical properties of steel fiber reinforced concrete with different strengths of concrete', Constr Build Mater, vol. 168, pp. 556–569, Apr. 2018, doi: 10.1016/j.conbuildmat.2018.02.164.

[4] D. S. Aliyu et al., 'Influence of polymer 3D printing on the durability and thermal performances of infrastructural buildings', in AIP Conference Proceedings, American Institute of Physics, Aug. 2024. doi: 10.1063/5.0218105.

[5] T. Wu, X. Yang, H. Wei, and X. Liu, 'Mechanical properties and microstructure of lightweight aggregate concrete with and without fibers', Constr Build Mater, vol. 199, pp. 526–539, Feb. 2019, doi: 10.1016/j.conbuildmat.2018.12.037.

[6] D. Y. Yoo and Y. S. Yoon, 'Structural performance of ultra-high-performance concrete beams with different steel fibers', Eng Struct, vol. 102, pp. 409–423, Nov. 2015, doi: 10.1016/j.engstruct.2015.08.029.

[7] J. H. Lee, B. Cho, and E. Choi, 'Flexural capacity of fiber reinforced concrete with a consideration of concrete strength and fiber content', Constr Build Mater, vol. 138, pp. 222–231, May 2017, doi: 10.1016/j.conbuildmat.2017.01.096.

[8] D. Y. Yoo, S. Kim, G. J. Park, J. J. Park, and S. W. Kim, 'Effects of fiber shape, aspect ratio, and volume fraction on flexural behavior of ultra-high-performance fiber-reinforced cement composites', Compos Struct, vol. 174, pp. 375–388, Aug. 2017, doi: 10.1016/j.compstruct.2017.04.069.

[9] M. Saridemir, 'Predicting the compressive strength of mortars containing metakaolin by artificial neural networks and fuzzy logic', Advances in Engineering Software, vol. 40, no. 9, pp. 920–927, 2009, doi: 10.1016/j.advengsoft.2008.12.008.

[10] P. Thamma and S. V Barai, 'Prediction of Compressive Strength of Cement Using Gene Expression Programming', in Applications of Soft Computing, J. Mehnen, M. Köppen, A. Saad, and A. Tiwari, Eds., Berlin, Heidelberg: Springer Berlin Heidelberg, 2009, pp. 203–212.

[11] I. B. Topçu and M. Saridemir, 'Prediction of compressive strength of concrete containing fly ash using artificial neural networks and fuzzy logic', Comput Mater Sci, vol. 41, no. 3, pp. 305–311, Jan. 2008, doi: 10.1016/j.commatsci.2007.04.009.

[12] G. Arslan and E. Cihanli, 'Curvature ductility prediction of reinforced High-strength concrete beam sections', Journal of Civil Engineering and Management, vol. 16, no. 4, pp. 462–470, Dec. 2010, doi: 10.3846/jcem.2010.52.

[13] P. Ramadoss, L. Li, S. Fatima, and M. Sofi, 'Mechanical performance and numerical simulation of high-performance steel fiber reinforced concrete', Journal of Building Engineering, vol. 64, Apr. 2023, doi: 10.1016/j.jobe.2022.105424.

[14] ACI 211, 'Standard Practice for Selecting Proportions for Normal', ACI Mater J, vol. 90, no. 3, 2009.

[15] A. ACI, '211.1-Standard Practice for Selecting Proportions for Normal', Heavyweight, and Mass Concrete, 2009.

[16] A. ACI, '211.1-Standard Practice for Selecting Proportions for Normal', Heavyweight, and Mass Concrete, 2009.

[17] T. S. Poole and P. J. Harrington, 'An Evaluation of the Maturity Method (ASTM C 1074) for Use in Mass Concrete 19970203 003 OTIC QUALITY HTBPSOi'iäS &', 1996.

[18] G. M. Giaccio I and V. M. Malhotra, 'Concrete Incorporating High Volumes of ASTM Class F Fly Ash', 1988. [Online]. Available: http://asmedigitalcollection.asme.org/cementconcreteaggregates/article-pdf/10/2/88/7073922/10_1520_cca10088j.pdf?casa_token=6gXxy0PzqGYAAAAA:vTf6E72p4Kwg-WUzv6QOqTL4rzX4rinNqXlU8WShv3zVjvfWc86FQIYZnQCJYoP5ddusHMQhqg

[19] D. S. Aliyu, S. I. Malami, F. H. Anwar, M. M. Farouk, M. S. Labbo, and S. I. Abba, 'Prediction of compressive strength of lightweight concrete made with partially replaced cement by animal bone ash using artificial neural network', in 2021 1st International Conference on Multidisciplinary Engineering and Applied Science, ICMEAS 2021, Institute of Electrical and Electronics Engineers Inc., 2021. doi: 10.1109/ICMEAS52683.2021.9692317.

[20] W. C. Liao, W. Perceka, and E. J. Liu, 'Compressive stress-strain relationship of high strength steel fiber reinforced concrete', Journal of Advanced Concrete Technology, vol. 13, no. 8, pp. 379–392, Aug. 2015,

doi: 10.3151/jact.13.379.
[21] M. Nili and V. Afroughsabet, 'Combined effect of silica fume and steel fibers on the impact resistance and mechanical properties of concrete', Int J Impact Eng, vol. 37, no. 8, pp. 879–886, Aug. 2010, doi: 10.1016/j.ijimpeng.2010.03.004.
[22] Z. Keshavarz and H. Torkian, 'Application of ANN and ANFIS Models in Determining Compressive Strength of Concrete', Journal of Soft Computing in Civil Engineering, vol. 2, no. 1, pp. 62–70, 2018, doi: 10.22115/SCCE.2018.51114.
[23] Y. M. Wang and T. M. S. Elhag, 'An adaptive neuro-fuzzy inference system for bridge risk assessment', Expert Syst Appl, vol. 34, no. 4, pp. 3099–3106, 2008, doi: 10.1016/j.eswa.2007.06.026.
[24] D. K. Sinha, R. Satavalekar, and S. Kasilingam, 'Application of Adaptive Neuro-Fuzzy Inference System for Evaluating Compressive Strength of Concrete', International Journal of Fuzzy Logic and Intelligent Systems, vol. 21, no. 2, pp. 176–188, 2021, doi: 10.5391/IJFIS.2021.21.2.176.
[25] J. S. R. Jang, 'ANFIS: Adaptive-Network-Based Fuzzy Inference System', IEEE Trans Syst Man Cybern, vol. 23, no. 3, pp. 665–685, 1993, doi: 10.1109/21.256541.
[26] M. A. Denaï, F. Palis, and A. Zeghbib, 'ANFIS based modelling and control of non-linear systems: A tutorial', in Conference Proceedings - IEEE International Conference on Systems, Man and Cybernetics, 2004, pp. 3433–3438. doi: 10.1109/ICSMC.2004.1400873.
[27] J. S. R. Jang, C. T. Sun, and E. Mizutani, 'Neuro-Fuzzy and Soft Computing-A Computational Approach to Learning and Machine Intelligence [Book Review]', IEEE Trans Automat Contr, vol. 42, no. 10, pp. 1482–1484, Apr. 2005, doi: 10.1109/tac.1997.633847.
[28] S. I. Abba et al., 'Emerging evolutionary algorithm integrated with kernel principal component analysis for modeling the performance of a water treatment plant', Journal of Water Process Engineering, vol. 33, Feb. 2020, doi: 10.1016/j.jwpe.2019.101081.
[29] O. Ünal, F. Demir, and T. Uygunoğlu, 'Fuzzy logic approach to predict stress-strain curves of steel fiber-reinforced concretes in compression', Build Environ, vol. 42, no. 10, pp. 3589–3595, 2007, doi: 10.1016/j.buildenv.2006.10.023.
[30] F. Bencardino, L. Rizzuti, G. Spadea, and R. N. Swamy, 'Stress-Strain Behavior of Steel Fiber-Reinforced Concrete in Compression', Journal of Materials in Civil Engineering, vol. 20, no. 3, pp. 255–263, 2008, doi: 10.1061/(asce)0899-1561(2008)20:3(255).
[31] W. C. Liao, W. Perceka, and E. J. Liu, 'Compressive stress-strain relationship of high strength steel fiber reinforced concrete', Journal of Advanced Concrete Technology, vol. 13, no. 8, pp. 379–392, 2015, doi: 10.3151/jact.13.379.
[32] F. Köksal, F. Altun, I. Yiğit, and Y. Şahin, 'Combined effect of silica fume and steel fiber on the mechanical properties of high strength concretes', Constr Build Mater, vol. 22, no. 8, pp. 1874–1880, 2008, doi: 10.1016/j.conbuildmat.2007.04.017.
[33] C. S. Poon, Z. H. Shui, and L. Lam, 'Compressive behavior of fiber reinforced high-performance concrete subjected to elevated temperatures', Cem Concr Res, vol. 34, no. 12, pp. 2215–2222, 2004, doi: 10.1016/j.cemconres.2004.02.011.
[34] M. Nili and V. Afroughsabet, 'Combined effect of silica fume and steel fibers on the impact resistance and mechanical properties of concrete', Int J Impact Eng, vol. 37, no. 8, pp. 879–886, 2010, doi: 10.1016/j.ijimpeng.2010.03.004.
[35] W. T. Lin, R. Huang, C. L. Lee, and H. M. Hsu, 'Effect of steel fiber on the mechanical properties of cement-based composites containing silica fume', J Mar Sci Technol, vol. 16, no. 3, pp. 214–221, 2008, doi: 10.51400/2709-6998.2010.